

## Evolution of surface morphology in Ni( $\gamma$ )/Ni<sub>3</sub>Al( $\gamma'$ ) two-phase foil during electrochemical etching

H.Y. Lee<sup>1,2,a</sup>, M. Demura<sup>2,b</sup>, Y. Xu<sup>2,c</sup>, D.M. Wee<sup>1,d</sup> and T. Hirano<sup>2,e</sup>

<sup>1</sup>Dept. of MSE, KAIST, 335 Gwahangno, Yuseoung-gu, Daejeon, 305-701, Korea

<sup>2</sup>National Institute for Materials Science, 1-2-1 Sengen, Tsukuba, Ibaraki, 305-0047, Japan

<sup>a</sup>dishy@kaist.ac.kr, <sup>b</sup>DEMURA.Masahiko@nims.go.jp, <sup>c</sup>XU.Ya@nims.go.jp, <sup>d</sup>wee@kaist.ac.kr,  
<sup>e</sup>HIRANO.Toshiyuki@nims.go.jp

**Keywords:** surface modification, two-phase alloy and electrochemical etching

**Abstract.** Evolution of surface morphology in Ni( $\gamma$ )/Ni<sub>3</sub>Al( $\gamma'$ ) two-phase foil of binary Ni-18 at.%Al was examined during the electrochemically selective etching in the electrolyte of distilled water including 1 wt.% (NH<sub>4</sub>)<sub>2</sub>SO<sub>4</sub> and 1 wt.% citric acid. In the early stage (0.5 h), only the  $\gamma$  matrix was etched and the outmost  $\gamma'$  particles were protected by a preexisting surface product. As the  $\gamma$  matrix was etched more, the side surfaces of the outmost  $\gamma'$  particles and the  $\gamma'$  particles that were located inside were exposed in the electrolyte. They were dissolved, and had a high density of fine dimples. However, the dissolution rate of the  $\gamma'$  particles was slower than that of the  $\gamma$  matrix and thus the selective etching was retained in this stage. Finally, at 5h, more  $\gamma'$  particles were exposed and the flat and smooth surfaces of the outmost  $\gamma'$  particles were completely eliminated by the dissolution on the side surfaces. From these observations plus the saturation of the current density observed in the electrochemical test, we concluded that the change in the surface morphology was finished at this stage. Thus, the surface became more rough and irregular, which resulted from the original two-phase microstructure and the fine dimple structure by transpassivation.

### Introduction

Intermetallic Ni<sub>3</sub>Al exhibits excellent high-temperature properties such as creep strength and oxidation/corrosion resistance [1]. Recently, its catalytic property has been revealed for hydrogen production reactions such as methanol decomposition [2-4] and methane steam reforming [5]. With these two kinds of beneficial properties, its foil or sheet, which has been successfully fabricated [6-8], can be used as a plate-type catalyst for a micro-channel chemical reactor to produce hydrogen.

The catalytic activity of Ni<sub>3</sub>Al can be improved by making the surface rough and irregular, which has been proved in a powder form [5]. For a foil form, we consider that the roughening of the surface can be achieved using two-phase microstructure combined with selective etching. That is, if a two-phase foil including Ni<sub>3</sub>Al phase is subjected to the selective etching that leaves only Ni<sub>3</sub>Al phase, the surface would become rough and irregular corresponding to its original microstructure. We here selected Ni( $\gamma$ )/Ni<sub>3</sub>Al( $\gamma'$ ) two-phase alloys, in which the size and distribution of the  $\gamma'$  particles can be controlled by cold rolling and subsequent heat treatment [9, 10]. The two-phase foil can be fabricated by cold rolling similarly to the Ni<sub>3</sub>Al single-phase foil [11, 12].

Regarding the selective etching, an electrochemical etching method is one of the best ways for precious control. We have confirmed that the electrochemical etching condition proposed by Mukherji et al. [13] is applicable for the selective etching of the  $\gamma$  matrix in the binary Ni( $\gamma$ )/Ni<sub>3</sub>Al( $\gamma'$ ) foils with various two-phase microstructures [14]. However, it has not yet to be clarified how the surface morphology changes with the progress of the etching, which knowledge is crucial to optimize this process.

In this paper, we thus examined the evolution of the surface morphology with the progress of the electrochemically selective etching in the binary Ni( $\gamma$ )/Ni<sub>3</sub>Al( $\gamma'$ ) two-phase foil. The foil heat-treated at 1273K was used since it included relatively large  $\gamma'$  particles, which were suitable for observation.

## Experimental

Ni( $\gamma$ )/Ni<sub>3</sub>Al( $\gamma'$ ) two-phase foil with the composition of binary Ni-18 at.%Al (thickness of 30  $\mu$ m) was fabricated by 98 % cold-rolling of a single crystalline ingot [6-8, 12]. It was heat-treated at 1273 K for 0.5 h in a flowing argon gas after evacuation to  $\sim 10^{-3}$  Pa and cut into square-type specimens of 10 x 10 mm.

The electrochemical etching test was conducted at 1.75 V for various etching times: 0.5, 3 and 5 h. The electrolyte was distilled water including 1 wt.% (NH<sub>4</sub>)<sub>2</sub>SO<sub>4</sub> and 1 wt.% citric acid. This electrolyte was selected according to the previous study by Mukherji et al. [13] and we have confirmed that this condition works for the selective etching of the  $\gamma$  matrix in the present foil [14]. The current density was monitored using a disc-type specimen with 14.5 mm in diameter in the same electrochemical condition. A conventional three-electrode system was used for the electrochemical etching tests, in which the specimen, a graphite rod and a saturated calomel electrode (SCE) were set as the working, the counter and the reference electrodes, respectively. The electrode potentials were referenced to the SCE. A potentiostat controlled with a computer (Hokuto Denko Corp., HZ-5000) was used.

The microstructure and the chemical composition were examined using a scanning electron microscope with a field-emission gun (SEM, Jeol, JSM-7000F) and energy dispersive X-ray spectrometer (EDS, Edax), respectively.

## Results

Fig. 1 and 2 show the surface morphologies of the specimens after the electrochemical etching for various times with lower and higher magnification, respectively. At 0.5 h, the  $\gamma$  matrix was selectively etched and the  $\gamma'$  particles were left behind as shown in Fig. 1(a). The  $\gamma'$  particles had heterogeneous size distribution that seemed bimodal: 0.5~1.5  $\mu$ m in the larger mode and 50~200 nm in the smaller mode. The exposed part of the larger ones was complicated polygonal and that of the smaller ones was

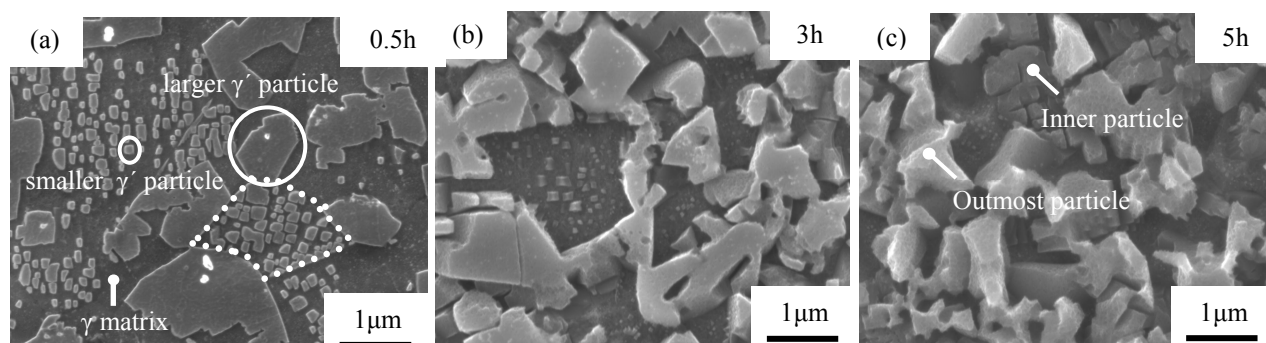


Figure 1. SEM images showing surface morphology of Ni( $\gamma$ )/Ni<sub>3</sub>Al( $\gamma'$ ) two-phase foils heat-treated at 1273 K for 0.5 h after the electrochemical etching at 1.75 V for (a) 0.5, (b) 3, (c) 5 h

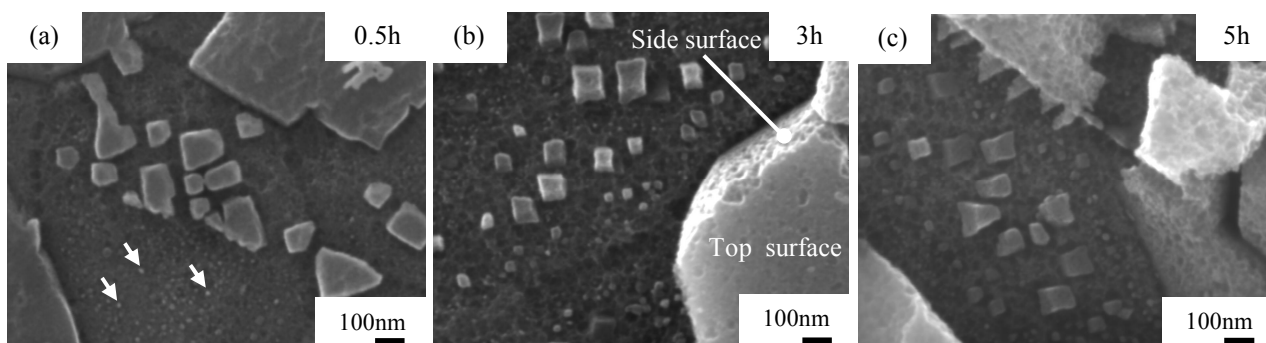


Figure 2. SEM images with high magnification showing surface morphology of Ni( $\gamma$ )/Ni<sub>3</sub>Al( $\gamma'$ ) two-phase foils heat-treated at 1273 K for 0.5 h after the electrochemical etching at 1.75 V for (a) 0.5, (b) 3, (c) 5 h

square or rectangular. This surface morphology exactly corresponded to the two-phase microstructure in which the larger and smaller  $\gamma'$  particles had a blocky shape and a nearly cuboidal shape, respectively [9]. It should be noted that the  $\gamma$  matrix was homogeneously etched, although the foil consisted of the recrystallized grains with the various crystallographic orientations [9]; for example, one of the grains is shown by the dotted lines in Fig. 1(a). This means that the dissolution rate of the  $\gamma$  matrix is independent on the crystallographic orientation.

At high magnification (Fig. 2(a)), it turned out that the surfaces of the  $\gamma'$  particles were flat and smooth, keeping their original state before the etching. That is, these  $\gamma'$  particles were located in the outmost surface layer. The high stability of these outmost  $\gamma'$  particles is probably due to a surface product formed in air or during the heat treatment in a flowing Ar gas. From the fact that the small particles of  $\sim 50$  nm stayed firmly without the detaching from the surface, the etching depth was estimated less than 50 nm at this moment. The etched  $\gamma$  matrix had a high density of fine dimples on the surface. This fine dimple structure was probably formed by transpassivation, where a passive oxide was broken down [15]. Besides, there were some small and bright particles with 10 nm or less in diameter as shown by the arrows, which might be  $\gamma'$  particles.

As the etching proceeded, the  $\gamma$  matrix was etched more, making the surface more rough and irregular (Fig. 1(b)). Regarding the outmost  $\gamma'$  particles, the top surface of them still kept the flatness, meaning that the preexisting surface product was highly protective. The side surfaces, however, showed a fine dimple structure similar with that appeared on the  $\gamma$  matrix, meaning that the dissolution occurred (Fig. 2(b)). In addition, the dissolution occurred on the inner  $\gamma'$  particles that were newly exposed in the electrolyte with the progress of the etching. Note that, in spite of these dissolutions of the  $\gamma'$  particles, the selectivity of the etching was still remained. That is, it was founded that the dissolution rate was intrinsically slower on the  $\gamma'$  phase, even without the protection by the preexisting surface product.

Finally, the outmost  $\gamma'$  particles changed its shape after 5 h and almost no flat surface was observed even on the top surfaces as shown in Fig. 1(c). Instead, the dimples were formed on all the surfaces (Fig. 2(c)). It was thus hard to find a trace of the state before the etching, and the original surface characteristic was completely removed by the etching. In addition to the change in the outmost particles, more  $\gamma'$  particles appeared from the inside by deep etching. These changes made the surface rough markedly; and the surface morphology seems close to that of skeleton metallic catalyst such as Raney Ni catalysts [16].

Table 1 lists the chemical composition obtained on the  $\gamma'$  particles and the  $\gamma$  matrix after the etching. Both  $\gamma$  matrix and  $\gamma'$  particles contained oxygen, indicating that the oxides were formed on the surface during the etching. Note that the oxygen content increased on the  $\gamma'$  particles with the etching time. Probably, it was related to the formation of Al oxide, which was highly stable and accumulated with the time. On the contrary, the oxygen content was almost constant on the  $\gamma$  matrix, suggesting that the formation rate of the oxides was equivalent to the dissolution rate.

Fig. 3 plots the current density as a function of the etching time. The current density represents the dissolution rate of the specimen. The values were scattered and thus normalized as shown by the thicker line. The current density, i.e. the dissolution rate was found to increase with the etching time until 3 h. Then, the increase in the current density became slower and finally it was virtually saturated

Table 1. The results of EDS analysis taken from the surface of the foils etched for 0.5, 3 and 5 h.

	0.5h			3h			5h		
	Ni	Al	O	Ni	Al	O	Ni	Al	O
$\gamma$	78.0 $\pm 0.4$	16.9 $\pm 0.1$	<b>5.1</b> $\pm 0.4$	79.0 $\pm 1.7$	16.0 $\pm 1.7$	<b>5.0</b> $\pm 1.0$	80.8 $\pm 2.8$	14.4 $\pm 2.3$	<b>4.8</b> $\pm 0.5$
$\gamma'$	71.3 $\pm 0.7$	22.9 $\pm 0.8$	<b>5.8</b> $\pm 0.1$	66.2 $\pm 0.1$	26.4 $\pm 0.1$	<b>7.4</b> $\pm 0.2$	65.8 $\pm 1.0$	27.0 $\pm 0.8$	<b>7.2</b> $\pm 0.3$

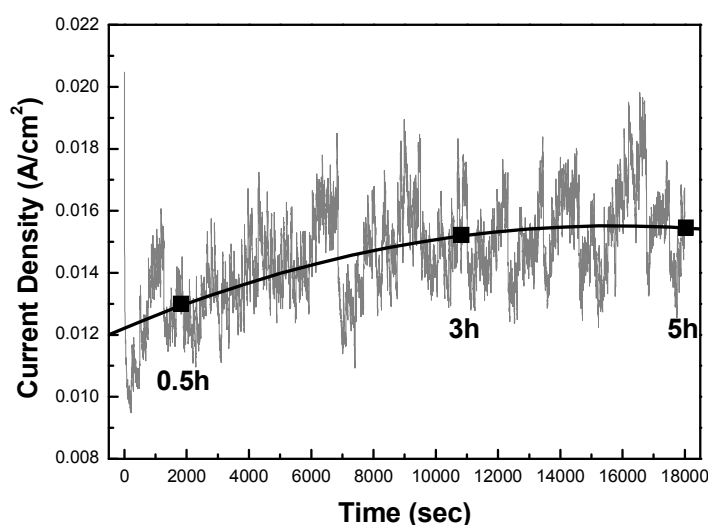


Figure 3. Current density during the electrochemical etching of Ni( $\gamma$ )/Ni<sub>3</sub>Al( $\gamma'$ ) two-phase foil heat-treated at 1273 K for 0.5 h as a function of the etching time.

at 5 h. This trend must correspond to the change in the surface morphology, which will be discussed in the next section.

## Discussion

The present results showed that the surface morphology changed with the etching time until 5 h. Fig. 4 shows the schematic diagram for the evolution of the surface morphology, where the small  $\gamma'$  particles are ignored for simplicity.

In the early stage (Fig. 4(b)), the roughening started by the selective etching of the  $\gamma$  matrix. The dissolution of the outmost  $\gamma'$  particles was prevented, which prevention is considered due to a preexisting surface product. Thus, the current density shown in Fig. 3 should correspond only to the dissolution of the  $\gamma$  matrix in this stage.

As the  $\gamma$  matrix was etched, the roughness became larger naturally, and the side surfaces of the  $\gamma'$  particles were newly exposed in the electrolyte (Fig. 4(c)). Interestingly, the dissolution occurred on this newly exposed side surfaces of the  $\gamma'$  particles (Fig. 2(b)), contrasting with the high stability of the top surfaces. This dissolution made the surface have the fine dimple structure. The same dissolution occurred on the surfaces of the newly exposed  $\gamma'$  particles, i.e. the inner ones, with the progress of the etching. These dissolutions of the  $\gamma'$  particles should contribute to the increase in the current density observed until 3 h. However, the dissolution rate was slower than that of the  $\gamma$  matrix, and thus the selective etching of the  $\gamma$  matrix was retained in this stage. That is, the cause of the selective etching was gradually shifted to the difference in the dissolution rate between  $\gamma$  matrix and  $\gamma'$

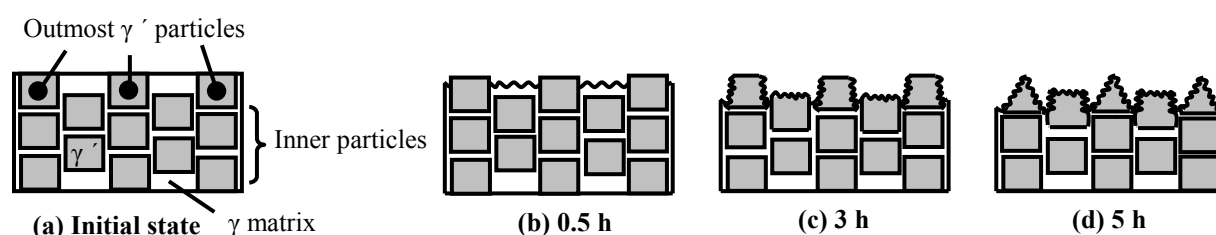


Figure 4. Schematic diagram showing the surface morphology change of Ni( $\gamma$ )/Ni<sub>3</sub>Al( $\gamma'$ ) two-phase foil heat-treated at 1273 K for 0.5 h during the electrochemical etching at 1.75 V as a function of the etching time.

particles. Regarding the fine dimple structure, it is considered to be formed by transpassivation. This fine dimple structure may be helpful to improve the specific surface area in addition to the effect of more coarse roughness corresponding to the two-phase microstructure.

Finally, after 5 h, the flat surfaces of the outmost  $\gamma'$  particles were eliminated by the dissolution on the side surfaces, and all the surfaces had the dimple structure (Fig. 4(d)). Thus, the characteristics in the original surface before the etching, i.e. the flatness and smoothness, disappeared completely. We can conclude that the change in the surface morphology was almost finished in this stage, which was supported by the saturation of the increase in the current density. Further evolution and surface modification cannot be expected by the etching for a longer time. In other words, the etching of 5 h is the optimum condition to obtain the most rough and irregular surface.

The above discussion revealed that the rough surface was formed from two mechanisms: the selective etching of the  $\gamma$  matrix and the transpassivation on the surface of the  $\gamma'$  particles. First, the selective etching, which yields the relatively coarse roughness corresponding to the two-phase microstructure, was mainly ascribed to the difference in the dissolution rate of each phase. An Al oxide can be assumed to play a crucial role for the difference in the dissolution rate. Our previous XPS analysis revealed that the Al oxide was formed only on the  $\gamma'$  phase but not on the  $\gamma$  phase in the present etching condition [17]. This Al oxide is stable and retards the dissolution of the  $\gamma'$  particles. This assumption is consistent with the chemical analysis indicating the accumulation of oxides on the  $\gamma'$  particles, probably the Al oxide, with the progress of the etching (Table 1). Besides, as a minor factor, the prevention by the preexisting surface product on the outmost  $\gamma'$  particles worked, especially in the early stage.

The second mechanism for the roughening was the transpassivation, yielding the fine dimple structure on the remained  $\gamma'$  particles. We consider that Ni-oxide was formed and dissolved through transpassivation on the surfaces of both phases, based on our previous XPS and potentiodynamic polarization results [17].

## Summary

The surface morphology of the Ni( $\gamma$ )/Ni<sub>3</sub>Al( $\gamma'$ ) two-phase foil was examined after the electrochemical etching for 0.5, 3 and 5 h and the following results were obtained.

1. The  $\gamma$  matrix was selectively etched and the  $\gamma'$  particles were left behind, yielding rough and irregular surface. The surface morphology was changed with the etching time: a number of the exposed  $\gamma'$  particles increased; and the roughening occurred on the surfaces of the  $\gamma'$  particles with a fine dimple structure. These changes made the current density increase until 3 h.
2. The flat and smooth top surfaces of the outmost  $\gamma'$  particles disappeared completely at 5 h, accompanied by the saturation of the increase in the current density. Thus, the surface change was completed at this stage.
3. The roughness was determined by two factors: the original two-phase microstructure and the fine dimple structure formed on the  $\gamma'$  particles. The former, relatively coarse roughness appeared by the difference in the dissolution rate, which can be related to the Al oxide existing only on the  $\gamma'$  particles. The latter, fine dimple structure was formed through transpassivation.

## Acknowledgment

This work was partly supported by the Korea Science and Engineering Foundation (KOSEF) grant funded by the Korean government (MOST) (No. R01-2007-000-10008-0). It was also supported by the Grant-in Aid for Scientific Research (C) (No. 19560774) from the Ministry of Education, Culture, Sports, Science and Technology (MEXT). The authors thank Mr. Takanashi for his helpful assistance in the foil preparation.

---

**References**

- [1] N.S. Stoloff, *Int. Mater. Rev.* Vol. 34 (1989) p.153
- [2] Y. Xu, S. Kameoka, K. Kishida, M. Demura, A.P. Tsai and T. Hirano, *Mater. Trans.* Vol. 45 (2004), p. 3177
- [3] D.H. Chun, Y. Xu, M. Demura, K. Kishida, M.H. Oh, T. Hirano and D.M. Wee, *Catal. Lett.* Vol. 106 (2006), p. 71
- [4] D.H. Chun, Y. Xu, M. Demura, K. Kishida, D.M. Wee and T. Hirano, *J. Catal.* Vol. 243 (2006), p. 99
- [5] Y. Ma, Y. Xu, M. Demura, D.H. Chun, G. Xie and T. Hirano, *Catal. Lett.* Vol. 112 (2006), p. 31
- [6] M. Demura, Y. Suga, O. Umezawa, E.P. George and T. Hirano, *Intermetallics* Vol. 9 (2001), p. 157
- [7] M. Demura, K. Kishida, Y. Suga and T. Hirano, *Metall. Mater. Trans. A* Vol. 33A (2002), p. 2607
- [8] M. Demura, K. Kishida, Y. Suga, M. Takanashi and T. Hirano, *Scrip. Mater.* Vol. 47 (2002), p. 267
- [9] M. Nakamura, M. Demura, Y. Xu and T. Hirano, *MRS proc.* 0980-II05-30 (2006)
- [10] M. Demura, S. Hata, K. Kishida, Y. Xu and T. Hirano, Unpublished work
- [11] H. Borodians'ka, M. Demura, K. Kishida and T. Hirano, *Intermetallics* Vol. 10 (2002), p. 255
- [12] D. Li, K. Kishida, M. Demura and T. Hirano, *Intermetallics* Vol. 16 (2008), p. 1317
- [13] D. Mukherji, G. Pigozzi, F. Schmitz, O. Nath, J. Rosler and G. Kostorz, *Nanotechnology* Vol. 16 (2005), p. 2176
- [14] H.Y. Lee, M. Demura, Y. Xu, D.M. Wee and T. Hirano, *MRS proc.* 1128-U05-35 (2008)
- [15] D.A. Jones, *Principles and prevention of corrosion* (Prentice Hall, USA 1996) p. 116-122
- [16] G. Ertl, H. Knozinger and J. Weitkamp, *Preparation of solid catalysts* (WILEY-VCH, Germany 1999) p. 28-43
- [17] H.Y. Lee, M. Demura, Y. Xu, D.M. Wee and T. Hirano, Unpublished work